



HAL
open science

A New Calcareous Nannofossil Record from the Lower Jurassic of Kermanshah, Western Iran: Implications for Biostratigraphy and Evolutionary Reconstructions

Abdi Asad, Emanuela Mattioli, Beatriz Bádenas

► **To cite this version:**

Abdi Asad, Emanuela Mattioli, Beatriz Bádenas. A New Calcareous Nannofossil Record from the Lower Jurassic of Kermanshah, Western Iran: Implications for Biostratigraphy and Evolutionary Reconstructions. *Geosciences*, 2022, 12 (2), pp.59. 10.3390/geosciences12020059 . hal-03860028

HAL Id: hal-03860028

<https://hal.science/hal-03860028v1>

Submitted on 18 Nov 2022

HAL is a multi-disciplinary open access archive for the deposit and dissemination of scientific research documents, whether they are published or not. The documents may come from teaching and research institutions in France or abroad, or from public or private research centers.

L'archive ouverte pluridisciplinaire **HAL**, est destinée au dépôt et à la diffusion de documents scientifiques de niveau recherche, publiés ou non, émanant des établissements d'enseignement et de recherche français ou étrangers, des laboratoires publics ou privés.

(Article)

A new calcareous nanofossil record from the Lower Jurassic of Kermanshah, western Iran: implications for biostratigraphy and evolutionary reconstructions

Abdi Asad ¹, Emanuela Mattioli^{2,3,*} and Beatriz Bádenas²

- ¹ Ferdowsi University of Mashhad, also at Zaminrizkavan Co. Ltd. Tehran, Iran; Asadabdi656@gmail.com
- ² Univ Lyon, UCBL, ENSL, UJM, CNRS, LGL-TPE, F-69622, Villeurbanne, France (emanuela.mattioli@univ-lyon1.fr)
- ³ Institut Universitaire de France (IUF)
- ⁴ Department of Earth Sciences, Faculty of Sciences, University of Zaragoza, 50009 Zaragoza, Spain (bbadenas@unizar.es)
- * Correspondence: Emanuela Mattioli (emanuela.mattioli@univ-lyon1.fr)

Abstract: Calcareous nanofossils are used here for the first time in order to establish a precise biostratigraphic framework for the Kermanshah radiolarite Formation, outcropping in Western Iran. The new data presented here challenge the previous tentative age interpretations (Pliensbachian to early Toarcian) based upon radiolarians. Calcareous nanofossil assemblages and events unequivocally indicate that the pelagic limestones and marls are late Sinemurian in age (NJT 3b nanofossil subzone), and that these are thrust over shales and cherts dated as uppermost Sinemurian (NJT 3b-c nanofossil subzone) and lowermost Pliensbachian (NJT 4 nanofossil zone). This result allows reconsideration not only of the age of the radiolarite formations, which are widespread in the Zagros orogenic system, but also a better understanding of the stratigraphic relationships between the various lithological units known in the area. Besides these new stratigraphic inferences, the calcareous nanofossil assemblages of the uppermost Sinemurian-lowermost Pliensbachian successions revealed the common presence of new morphologies of the *Mitrolithus* genus, never described before. These findings allow the description of three new species, *M. montgolfieri*, *M. pseudonannoconus*, and *M. tethysiensis*, and reveal the existence of homeomorphy between the spine structure of conical Lower Jurassic coccoliths and the widespread Cretaceous nannoconids.

Keywords: calcareous nanofossils, biostratigraphy, taxonomy, Lower Jurassic, Kermanshah radiolarite Basin, West Iran

1. Introduction

The Lower Jurassic Kermanshah radiolarite Formation crops out in West Iran within the Zagros orogenic system, which extends from South-West Iran to North Iraq. This mountain chain was produced by the collision between the Arabian Plate and the Cimmerian Block in Central Iran. From a paleogeographic point of view, the Kermanshah Basin was located to the north-east of the Arabian continental platform and was separated from the Neo-Tethys Ocean by the Bisotoun shallow-carbonate platform (Fig. 1a–c). The studied sections in the Kermanshah area are composed of shales, limestones and cherts or radiolarites, with intercalated pyroclastic, oolitic/bioclastic packstone/grainstone and calciturbidite deposits. These sediments were previously dated as Pliensbachian–Aalenian [1], based on a few samples where radiolarians were recorded. Namely, the recovery of *Præconocaryomma bajaensis* sp. and *Bagotum modestum* sp. in the lowermost part of the limestone-dominated member provided a Pliensbachian or early Toarcian age determination (Pessagno and Whalen, in Carter et al. [2]). Within the ribbon chert-dominated member, the presence of *Katroma* sp. in its lowermost part provided an age older than early Toarcian [3], whereas *Elodium* sp. in its upper part indicated a Toarcian and Aalenian age [3]. However, because of the wide range of radiolarian taxa and the scarcity and poor

Citation: Abdi, A.; Emanuela, M.; Beatriz, B. A new calcareous nanofossil record from the Lower Jurassic of Kermanshah, western Iran: implications for biostratigraphy and evolutionary reconstructions. *Geosciences* **2022**, *12*, x. <https://doi.org/10.3390/xxxxx>

Academic Editor: Firstname Last-name

Received: date

Accepted: date

Published: date

Publisher's Note: MDPI stays neutral with regard to jurisdictional claims in published maps and institutional affiliations.



Copyright: © 2021 by the author. Submitted for possible open access publication under the terms and conditions of the Creative Commons Attribution (CC BY) license (<https://creativecommons.org/licenses/by/4.0/>).

preservation of radiolarian findings (most of fossil specimens have undergone calcite replacement in Kermanshah area sediments), additional biostratigraphic data are required in order to accurately dating these Lower Jurassic successions.

For this purpose, a detailed analysis of calcareous nannofossil content has been undertaken in the Kermanshah sedimentary successions. Although a significant number of the selected samples are barren in nannofossils, some levels have delivered a rich nannofossil assemblage which allowed precise dating of some parts of the succession. Published Jurassic nannofossil zonal schemes (e.g., Barnard and Hay [4], Hamilton [5],[6], Medd [7], Bown [8], Bown et al. [9], Mattioli and Erba, [10], Ferreira et al. [11]) are based on successions in North and West Europe, and other (mainly Tethyan) areas in the Northern Hemisphere. The few published records of Lower Jurassic nannofossils from the South-East Tethys come from Sulawesi [12] or Timor [8] or from offshore North-West Australia[13], and are very scattered.

The new biostratigraphic framework for the Lower Jurassic in the Kermanshah area presented in this paper allows a more precise dating of the Kermanshah radiolarite Formation. The new nannofossil data are also relevant because very few studies on calcareous nannofossils are available from such Lower Jurassic, low-latitude sites located much more to the east than the well-known western Tethys sites. In addition, some samples of the Kermanshah Formation revealed new nannofossil species never documented before of the genus *Mitrolithus*, a typical Tethyan Lower Jurassic taxon.

2. Geological context of the studied succession

According to palaeogeographic reconstructions, the Kermanshah radiolarite Basin (western Iran) developed during the Mesozoic Era at the western border of the central Neo-Tethys Ocean and northeast of the Arabian platform located at the eastern edge of Gondwana [14]–[19] (Fig. 1a, b). More specifically, the Kermanshah Basin successions are exposed in the Crush zone or High Zagros Belt (HZB in Fig. 1c), within the Zagros orogenic system. The earliest extensional phase, which marks the opening of the Kermanshah Basin, occurred during the Late Triassic (e.g. [20]). The rifting continued through the Jurassic [18],[21], and the tectonic inversion generating the Zagros orogenic system began in the Late Cretaceous. The latter phase originated in response to the obduction of Tethyan oceanic lithosphere onto the Arabian passive margin, and to the collision between the Arabian Plate and the Central Iran Cimmerian Block [20]–[23].

The High Zagros Belt includes four geological units (Fig. 1d): the Bisotoun limestones, belonging to the Bisotoun carbonate platform, which separated the Kermanshah Basin from the Arabian continental platform [1],[18],[22]–[24] (Fig. 1e); a transition zone between the Bisotoun limestone and the Kermanshah deposits; the Kermanshah Basin succession; and the Neo-Tethys ophiolitic obduction nappe [18],[25],[26] (Fig.1c).

A variety of marine sedimentary rocks, including radiolarites, pelagic limestones, shales and event deposits (pyroclastic deposits, internalites, calciturbidites, and debris flows) accumulated in the Kermanshah Basin during the Mesozoic [17],[23],[27]. Our work focused on two section, ~2 km apart, in the Karmanshah area: the Kani Sad (34° 19' 11" N and 47° 02' 04" E) and Sad sections (34° 19' 11.1" N and 47° 02' 03.8" E). The Kani Sad section was previously studied by Abdi et al. [1],[23],[24] who presented the stratigraphic and sedimentological framework of the outcropping units. Three Lower Jurassic informal lithological members, dated as Pliensbachian to Aalenian based on radiolarian record, were differentiated (Table 1): J.1, mainly including cherts; J.2, formed by pelagic limestones with marl intercalations and event deposits (internalites, pyroclastic deposits); and J.3, mainly consisting of ribbon cherts (i.e., chert-shale alternations). The Kani Sad and Sad

sections studied in this work include part of the described successions in Abdi et al. [1],[23],[24], but new biostratigraphic data have allowed an improved stratigraphy of the units and have obliged us to rename provisionally some of them, waiting for future new biostratigraphic data and formal lithostratigraphic definition (Table 1). In particular, the studied succession encompasses two lithological members, named here J.0 and J.1 based on present outcrop position (Fig. 2). The J.0 member is dominated by shales and cherts with intercalated pyroclastic deposits and calciturbidites (calcarenites), and partly coincides with the J.1 member (cherts) of Abdi et al. [1]. In the Kani Sad and Sad sections, this member is 12 m and 6 m thick, respectively. The J.1 member is 20 m thick and outcrops in the Kani Sad section, and it coincides with J.2 unit (pelagic limestones with marl intercalations) described by Abdi et al. [1],[23],[24], which was previously dated by radiolarian fossils as Pliensbachian pro parte to early Toarcian.

As the shaley units of the J.0 member of the Kani Sad and Sad sections are part of two limbs of a syncline here (see Results section below) indicate that in fact J.0 is younger in age than J.1, so that J.1 is thrust over J.0 (Fig. 2; Table 1).

3. Nannofossil sampling and analysis

A total of 77 samples were studied for calcareous nannofossils. Samples come from the carbonate-rich beds, namely: 23 samples from J.0 unit (14 from the Kani Sad section and 9 from the Sad section), and 54 samples from the J.1 unit in the Kani Sad section (Fig. 2; Table 2). Smear slides were prepared following the method described in Bown and Young [28]. For each rock sample, a small amount of powdered rock was mixed with a drop of water and spread onto a cover slide; the water was evaporated on a hot plate, then the slide was mounted on a microscope slide using Rhodopas B resin (polyvinyl acetate). The slides were observed using a Leica DM750P polarizing microscope, with a 1000X magnification. Three transverses of each slides were systematically scanned (a surface of approximately 19.2 mm²) and all the encountered calcareous nannofossils were counted. Preservation of nannofossils was evaluated according to the criteria of etching and overgrowth described by Roth [29]. Semi-quantitative abundance classes were calculated (rare, few, common and abundant) according to the species and specimen abundance in a single field of view [28].

Taxonomy of the studied specimens was based on the seminal work of Bown [8] for muroliths (i.e., coccoliths characterised by a simple structure with calcite elements of the distal shield extending vertically, representing the earliest coccoliths to have appeared in the Late Triassic; [8]). For placoliths (i.e., coccoliths composed of two shields which lie on top of one-another, and are connected by a central tube; the two shields show radial calcite elements; Bown [8]), the taxonomy of de Kaenel and Bergen [30] and Mattioli et al. [31] was used.

For biostratigraphy, the following standard zonations were used: Bown [8], updated by Bown and Cooper [32] for the North-West Tethys areas (especially England, Germany and Austria); Mattioli and Erba [10] for the South-West Tethys (mainly central and northern Italy, and South-East France); and Ferreira et al. [11] for the proto-Atlantic region (Portugal).

4. Results

4.1. Calcareous nannofossil biostratigraphy

In the stratigraphically lower part of the Kani Sad section (J.1 member, thrust over the J.0 member; Table 1 and Fig. 2), 39 of the 54 samples are barren of nannofossils, and the remaining samples yield poorly preserved and low diversity nannofossil assemblages.

141 However, the productive samples include biostratigraphically useful taxa, including *in-*
142 *certae sedis* *Schizosphaerella* spp. and the coccoliths *Mitrolithus elegans*, *M. lenticularis*, *M.*
143 *jansae*, *Parhabdolithus robustus* and, sporadic *P. marthae* (amongst other coccoliths), with
144 abundances varying from rare to few (1 specimen in 31–150 fields of view to 1 specimen
145 in 15–30 fields of view).

146 In the stratigraphically upper part of the Kani Sad section (J.0 member), most of the sam-
147 ples bear nannofossils, and display a relatively richer assemblage as some species (like *M.*
148 *elegans*) are few-to-common in discrete levels. This interval is also biostratigraphically rel-
149 evant because it includes the first occurrence (FO) of bi- and three-shielded placoliths,
150 namely *Similiscutum avitum* in sample J.0-9 and *S. orbiculus* in sample J.0-18, and of *Maza-*
151 *ganella pulla* in sample J.0-1. These occurrences are particularly relevant because they al-
152 low the correlation of the Kermanshah section with other stratigraphically well-con-
153 strained sections of the western Tethys (see discussion). The J.0 member in the Sad section
154 (reversed portion underlying the over-thrust; Fig. 2; Table 2) revealed the richest nan-
155 nofossil content with several species of the genus *Mitrolithus* being common in the slides.
156 Species of *Similiscutum* also occur although discontinuously along with *M. pulla* and *M.*
157 *protensa*. *Parhabdolithus marthae* likely last occurred (LO) in this interval (sample J.0-28).

158 The most striking feature of the nannofossil assemblages in the stratigraphically upper
159 parts of the Kani Sad and Sad sections is the morphological diversity of the genus *Mitro-*
160 *lithus* (black stars in Fig. 2). In particular, a huge variability was observed for *Mitrolithus*
161 *elegans*, which is a basket-shaped murolith-coccolith, slightly flaring in side view, charac-
162 terized by a spine that is narrow at its base, broadening out and rounding off at its top.
163 This form may occur as entire coccoliths or as isolated spines. Detached spines are circular
164 in plan-view and have been described as a separate species (*Alvearium dorsetense* Black,
165 [33]). These coccoliths recorded in the in J.0 member bearing very developed spines with
166 peculiar morphologies have been described as new species here (see taxonomic section
167 below).

168 4.2. Taxonomy of new *Mitrolithus* species

169 The genus *Mitrolithus* is a typical Lower Jurassic taxon, currently represented by
170 three species, namely *M. elegans* (the type species), *M. jansae* and *M. lenticularis*. The mor-
171 phological characters of the three *Mitrolithus* species are illustrated in Figure 3. The com-
172 mon and morphologically diverse assemblage of *Mitrolithus* observed in the Kermanshah
173 area contains the three species, as well as previously undescribed types, which are mor-
174 phologically similar to *M. elegans*. However, significant differences in the spine and coc-
175 colith size and shape justify the introduction of new species.

176 Deflandre in Deflandre and Fert [34] (p. 148) erected the genus *Mitrolithus* and de-
177 scribed it as "Discolithe en cuvette dont le centre porte une protubérance massive évasée,
178 d'allure fongiforme, donnant à la vue latérale l'aspect d'une mitre" ("A bowl-shaped dis-
179 colith the central area of which bears a massive flaring mushroom-shaped protuberance,
180 giving the lateral view the appearance of a mitre", after Young et al. [35]). Bown and
181 Young in Young et al. [35] (p. 129) emended the diagnosis of *Mitrolithus* as follows: "Coc-
182 coliths with an outer rim of thin, broad calcite laths orientated perpendicular to the base
183 and tangential to the ellipse. The central area is filled by a massive boss or spine consisting
184 of several superimposed cycles of radial calcite elements. The spine sits in the coccolith
185 rim on an inner cycle of elements and is attached via a narrow, hollow spine base".

186 *Mitrolithus elegans* (Fig. 3A) was first described by Deflandre in Deflandre and Fert
187 [34] (p. 148) as: "Cuvette, en vue latérale, un peu évasée, surmontée d'une masse d'abord
188 étroite, puis élargie et arrondie au sommet", which can be translated into "Basket-like dis-
189 colith slightly tapering in side view, surmounted by a protuberance narrow at its base and
190 flared upwards, ending up with a rounded top." The prominent distal rim cycle is com-
191 posed of tangential rectangular elements, which are vertically arranged to form a tall,
192 basket-like structure. The proximal rim cycle is composed of prismatic elements infilling
193 the central area around a central hole, which is the base of the hollow spine. The proximal

rim cycle elements have a distal extensions forming an inner cycle lower than the distal rim cycle, thus having a canine-teeth shape in side view against the inner surface of the distal rim cycle. The spine originates from the coccolith base as a narrow tube inside the coccolith basket, then flares out from the coccolith rim with a diameter larger than that of the coccolith rim. Its upper surface is domed. The spine is thus lenticular in cross-section, circular in plan-view, and composed of flat, superimposed wedge-shaped elements. Such elements have a plate c-axis, tangential to the longitudinal axis of the spine. Detached spines do occur very often, and have been described as *Alvearium dorsetense* [33].

The second species of *Mitrolithus* recorded in the Kermanshah area is *M. jansae* (Fig. 3B). The earliest paper to describe this species was Prins [36] who used the name *Mitrolithus irregularis*. This name was invalid because Prins presented a very clear drawing (Fig. 3B-5), but the species was not formally described with a designated holotype. Later, Wiegand [37] (p. 1152) described this species as *Calcivascularis jansae*, having the characteristics of the genus, namely: "A basket shaped nannolith filled with a core consisting of many radially arranged elements". Eventually, Young et al. [35] suggested that the specific name *jansae* should stand as the first valid description of the coccolith, but the genus *Calcivascularis* is redundant, because *M. elegans* and *M. jansae* appear to be very closely related, and the genus *Calcivascularis* is otherwise monospecific. Bown and Young in Young et al. [35] (pp. 130-131) thus recombined *Calcivascularis jansae* into *Mitrolithus jansae*, having exactly the same characteristics of the genus *Mitrolithus*. The rim of *M. jansae*, composed of rectangular elongated elements, has a narrow truncated-cone shape, slightly elliptical in cross-section. The spine (or core in the original diagnosis) is lodged within the rim, and is constructed of several superimposed cycles, each composed of radial elements. The overall structure of the coccolith is very bulky and the spine/core is mostly enclosed by the coccolith rim. A high degree of rim height variability has been observed [38] (plate 1, fig. 27). The coccolith is often observed in side view and more rarely in proximal/distal view. In such specimens, the radial-elements of the spine are well visible. In very overgrown specimens, the rectangular laths of the distal shield can be enlarged and form a rosette-like structure in proximal view surrounding the core. Such poorly preserved specimens have been figured as *Rucinolithus* sp. by Casellato and Erba [38] (plate 2, fig. 16-17).

The third species of *Mitrolithus* recorded in the Kermanshah area is *M. lenticularis* (Fig. 3C). Bown [8] (p. 28) introduced the species, *Mitrolithus lenticularis*, which possesses "... a spine which completely fills the central area and has a domed upper surface which coincides with the rim top; the spine is irregularly structured and oval in plan-view." *Mitrolithus lenticularis* is distinguished from *M. elegans* by its smaller size, lower distal shield rim, and a domed-spine never higher than the distal shield. The spine is therefore included within the coccolith rim and detached spines are not observed. Overall, *M. lenticularis* has a rugby-ball shape and can be often observed tilted, rather than in side or proximal/distal view.

Bown [8] relates that a number of specimens from Timor (Indonesia) resembling to *M. elegans* displayed a noticeable "elevation of the spine due to an increased number of superimposed rings of equal diameter forming a broad, parallel-sided column before terminating in the domed top" (plate 3, figs. 14-15). Similar specimens occur abundantly in Kermanshah area, in the uppermost Sinemurian or lowermost Pliensbachian, of both the Kani sad and Sad sections. Such specimens along with some other peculiar coccoliths are herein described as three new *Mitrolithus* species.

Mitrolithus montgolfieri sp. nov. Mattioli in Abdi et al.

Figure 4, micrographs A(1-4), text-figure A(5)

Diagnosis. A species of *Mitrolithus* with a relatively small basket-like rim and a large boss/spine resting on the distal side of the rim. The spine possesses a very typical hot-air balloon shape, made of radially arranged elements forming a globular, hollow space in its center.

248 Description. A coccolith with a protolith rim structure quite similar to that of *M. elegans*,
249 but slightly narrower and smaller (see holotype dimensions below). The central area
250 is reduced and surmounted by a bulbous spine resting on the rim. The basket-like rim is
251 small relative to the spine. This latter typically presents an empty globular cavity in its
252 center.

253 Dimensions of the holotype. Coccolith rim length: 5.4 μm ; coccolith rim height: 2.8
254 μm ; coccolith rim plus spine height: 6.2 μm .

255 Differentiation. *Mitrolithus montgolfieri* sp. nov. differs from *M. elegans* because of the
256 smaller dimensions of the basket-like rim and, mainly, for the very peculiar structure of
257 the spine. It differs from *M. jansae* because of the more reduced height of the rim and from
258 *M. lenticularis* because of the narrower basket-like rim and the bulbous spine flaring from
259 it.

260 Derivation of name. From the Montgolfier brothers, inventors of the hot-air balloon,
261 referring to the spine shape.

262 Holotype. Figure 4A-1, sample J.0-28. Repository: Collections de Géologie de Lyon,
263 FSL N° 769033.

264 Type level. Uppermost Sinemurian, sample J.0-28, J.0 informal lithological member.

265 Type locality. Iran, Sad section (34° 19' 11.1" N and 47° 02' 03.8" E).

266 Occurrence. Type material, uppermost Sinemurian.

267
268 *Mitrolithus pseudonannoconus* sp. nov. Mattioli in Abdi et al.

269 Figure 4, micrographs B(1-5), text-figures B(6)

270
271 Diagnosis. A species of *Mitrolithus* with a very low rim and a prominent, flaring
272 spine, made of radial elements, longitudinally crossed by a well-distinguished canal.

273 Description. *Mitrolithus pseudonannoconus* sp. nov. possesses a basket-like rim very
274 reduced in size, closely placed against the prominent spine. The rim can be sometimes
275 extremely low, and poorly visible at the base of the spine (Fig. 4B 1-5). The spine possesses
276 a structure flaring distally and is flat at its top. The radial calcite elements forming the
277 spine delineate an axial canal, which is easily visible in optical microscope. Isolated spines
278 do occur, which can be misleading as they closely resemble the morphology of a *Nanno-*
279 *conus* with intermediate-sized axial canal.

280 Differentiation. *Mitrolithus pseudonannoconus* sp. nov. is a very distinctive forms of
281 *Mitrolithus*, which differs from all the other species because of the very reduced dimen-
282 sions (height) of the basket-like rim and for the peculiar structure of the spine, which is
283 multi-layered and with a trapezoidal shape in side view.

284 Remarks. There is morphological transition from specimens with a reduced basket-
285 like rim, until this is extremely reduced and sometimes lacking. Those specimens look
286 very similar to *Nannoconus* with intermediate-sized axial canal.

287 Derivation of name. From the greek $\psiευδής$ (pseudes) meaning false, and *Nannoco-*
288 *onus*, the Cretaceous nannoliths.

289 Dimensions of the holotype. Coccolith rim length: 2.9 μm ; coccolith rim height: 1.1
290 μm ; coccolith rim plus spine height: 5 μm .

291 Holotype. Figure 4B-1, sample J.0-26. Repository: Collections de Géologie de Lyon,
292 FSL N° 769031.

293 Type level. Uppermost Sinemurian, sample J.0-26, J.0 informal lithological member.

294 Type locality. Iran, Sad section (34° 19' 11.1" N and 47° 02' 03.8" E).

295 Occurrence. Type material, uppermost Sinemurian.

296
297 *Mitrolithus tethysiensis* sp. nov. Mattioli and Bown in Abdi et al.

298 Figure 4, micrographs C(1-6, 8), text-figure C(7)

299
300 1987 *Mitrolithus elegans* Bown [8], pl. 3, figs. 14, and 15

301

Diagnosis. A *Mitrolithus* species, with a very prominent spine due to an increased number of superimposed cycles of elements forming a broad, parallel-sided column before terminating in a domed top.

Description. A large coccolith, with a typical *Mitrolithus*, basket-like rim, surmounted by a very large boss/spine mostly resting on the inner rim cycle. The spine is raised above the rim, because (like for *M. elegans*) the spine base is narrow before flaring out distally. The spine is very thick in side view, with superimposed series of radial elements surrounding a narrow axial-canal.

Differentiation. This is a very distinctive *Mitrolithus* species, very different from the other *Mitrolithus* species because of the peculiar shape of its spine.

Remarks. Bown [8] reported similar specimens from a Timor sample (J237), and interpreted them as a *M. elegans*, because of the quite similar coccolith architecture. However, he noticed the very peculiar, multi-layered spine, that justify the introduction of a new species.

Derivation of name. From Tethys Ocean, because the two localities where this new species has been recorded (Timor and Iran) are located in eastern Tethys.

Dimensions of the holotype. Coccolith rim length: 4.1 μm ; coccolith rim height: 2.1 μm ; coccolith rim plus spine height: 6.95 μm .

Holotype. Figure 4C-1, sample J.0-28. Repository: Collections de Géologie de Lyon, FSL N° 769033.

Type level. Uppermost Sinemurian, sample J.0-28, J.0 informal lithological member.

Type locality. Iran, Sad section (34° 19' 11.1" N and 47° 02' 03.8" E).

Occurrence. Type material, uppermost Sinemurian.

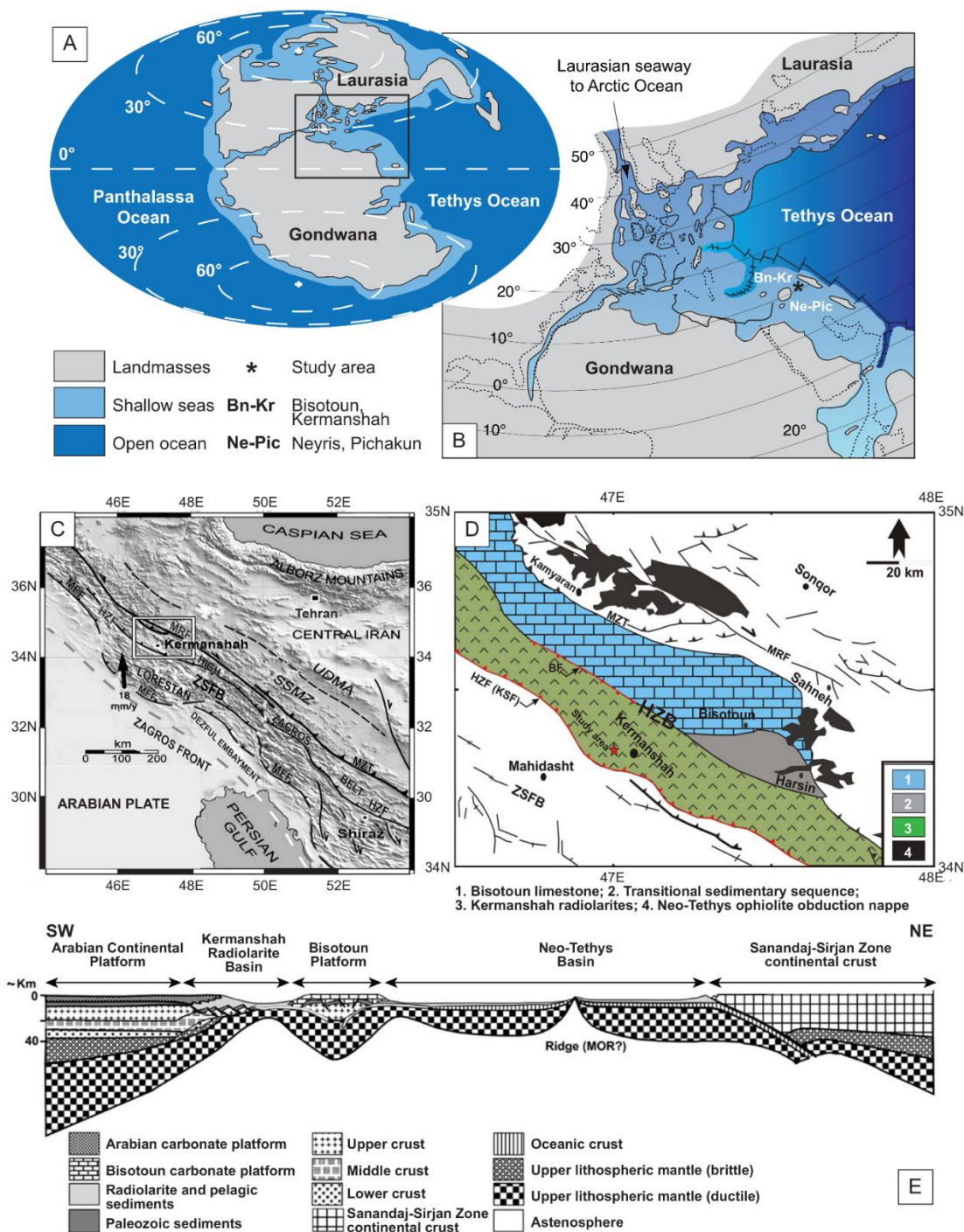


Figure 1. (A) Paleogeographic map of Lower Jurassic (modified after Blakey,[52]). (B) Paleogeography of the western Tethys with location of the studied Kermanshah Radiolarite Basin (modified after Bassoulet et al. [15]). (C) Regional map of the Zagros fold-and-thrust belt, indicating the location of the studied area of Kermanshah in West Iran (see rectangle). Topography comes from <http://edc.usgs.gov>. (D) Simplified geological map indicating the main tectonostratigraphic domains and showing the position of the studied section near Kermanshah (red star) in the High Zagros Belt (HZB). The Kermanshah radiolarite outcrops are limited by the Bisotoun Fault (BF) to the North and the Kuh-e-Sefid Fault (KSF = HZF) to the South (after Abdi et al. [1], and Navabpour et al. [18], modified). (E) Sketch showing the cross-section from the Arabian continental platform to the Sanandaj-Sirjan active margin for the Early Jurassic, with the location of the Kermanshah radiolarite Basin. The latter which was separated from the Neo-Tethys Basin by the Bisotoun carbonate platform (modified from Wrobel-Daveau et al. [22]).

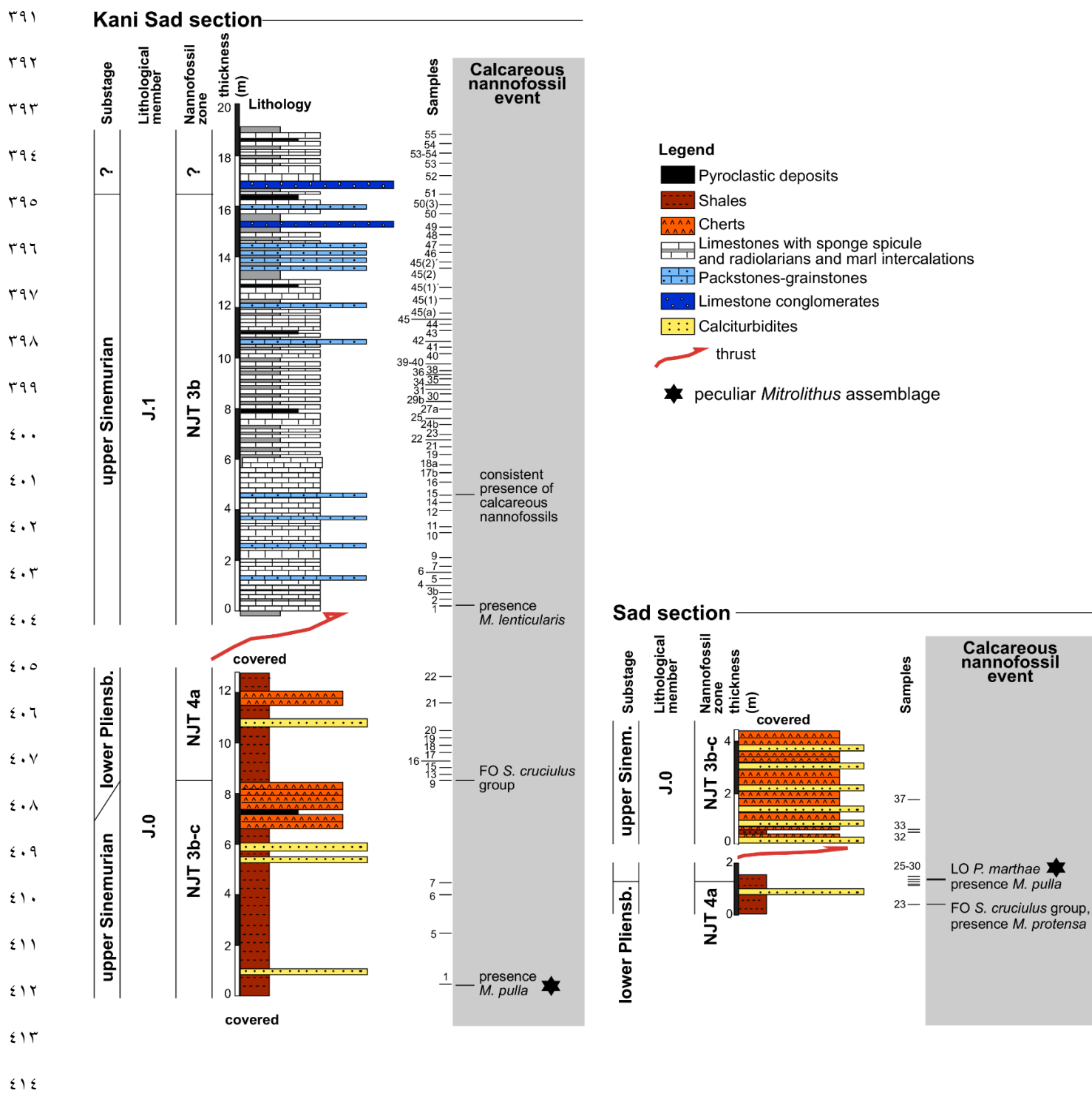
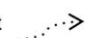


Figure 2. Stratigraphic logs of the Kani Sad and Sad sections indicating the position of nannofossil samples (partly modified after Abdi et al. [1],[23],[24]). The FO of the *S. cruciulus* group is reported, as *Similiscutum cruciulus*, *Similiscutum orbiculus* and *Similiscutum avitum* likely represent different ecophenotypes of the same species (Mattioli et al. [39]). Note that, according to nannofossil biostratigraphy, the J.0 member of the Kani Sad and Sad sections is younger than the J.1 member. The shaly units of the J.0 member of the Kani Sad and Sad sections are part of two limbs of a syncline structure, which is over-thrusted by the siliceous mudstones and grainstones of the J.1 member. The lower part of the Sad section is stratigraphically reversed, as also shown by the position of nannofossil zones.

Table 1. Synthesis of the stratigraphic members described in the studied Kermanshah area in previous and present work.

Kani Sad section (Abdi et al., 2014, 2016)			Present paper				
Lithological member	Thickness and dominant lithology	Age	Kani Sad and Sad sections and nannofossil zones (present tectonic position)		Restored position and age		
J.3	22 m, ribbon cherts	Middle Toarcian-Aalenian	Not studied				
J.2	18 m, limestones with marl intercalations	Pliensbachian p.p.-early Toarcian	J.1 20 m, limestones with marl intercalations	NJT 3b-c	J.0	NJT 4a	Lower Pliensbachian
J.1	3 m, cherts		J.0 up to 12 m, cherts, shales and calciturbidites	NJT 4a	uncertain interval		Upper Sinemurian
				NJT 3c	J.1	NJT 3b	

thrust 

probable fault contact 

420
426
427
428
429
430
431
432
433
434
435
436
437
438
439
440
441
442
443
444
445
446
447
448
449
450
451
452
453
454
455
456
457
458
459
460
461
462
463
464
465
466
467
468
469
470
471
472
473
474
475
476
477
478
479

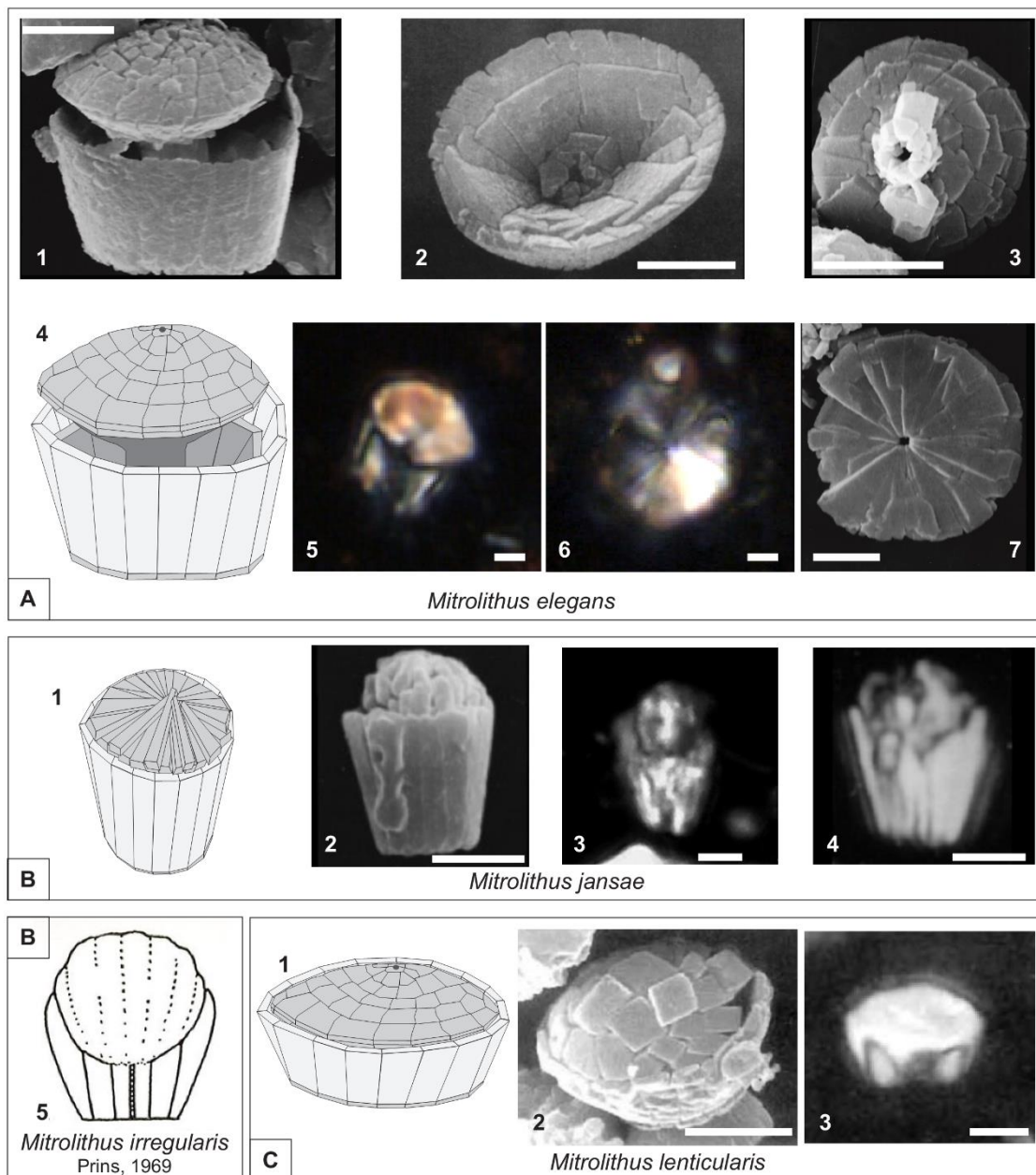


Figure 3. The three species of *Mitrolithus* known nowadays, as represented in the literature with schematic drawing illustrating their main morphological features. The white scale bar is 2 μm .

(A) *Mitrolithus elegans*: 1. SEM image of a side-view coccolith, after Bown [8] (plate 3 fig. 7); 2. SEM image of a distal-view coccolith without the spine (Bown [53], plate 3 fig. 1); 3. SEM image of an isolated spine, proximal view (the broken spine is still visible), after Bown [8] (plate 3 fig. 10); 4. Sketch redrawn from the SEM image in 1. 5. A side-view specimen recorded in the Kermanshah area (sample J.0-28) under optical microscope, crossed polars. 6. An isolated spine in distal view recorded in the Kermanshah area (sample J.0-28) under optical microscope, crossed polars. 7. SEM image of an isolated spine, distal view, after Bown [8] (plate 3 fig. 12).

(B) *Mitrolithus jansae*: 1. Sketch redrawn from SEM images; 2. SEM image of a side-view coccolith, after Bown and Cooper [51] (plate 1 fig.11); 3. A side-view specimen under optical microscope, crossed polars after Menini et al. [54] (plate 1 fig. 14). The calcite laths forming the distal shield appear light grey, while the highly birefringent elements inside these laths, as high as the 2/3 of the rim, likely correspond to the proximal shield elements, which are rarely visible due to the bulky structure of the coccolith; 4. A side-view specimen under optical microscope, crossed polars, after Bown and Cooper [32] (plate 1 fig. 16); 5. The sketch of *M. irregularis* figured as *nomen nudum* by Prins [36] and interpreted as it was derived from *M. elegans*.

(C) *Mitrolithus lenticularis*: 1. Sketch redrawn from SEM images; 2. SEM image of a side/distal-view coccolith (holotype), after Bown [8] (plate 4 fig. 7); 3. A side-view specimen under optical microscope, crossed polars after Bown [8] (plate 12 fig. 29).

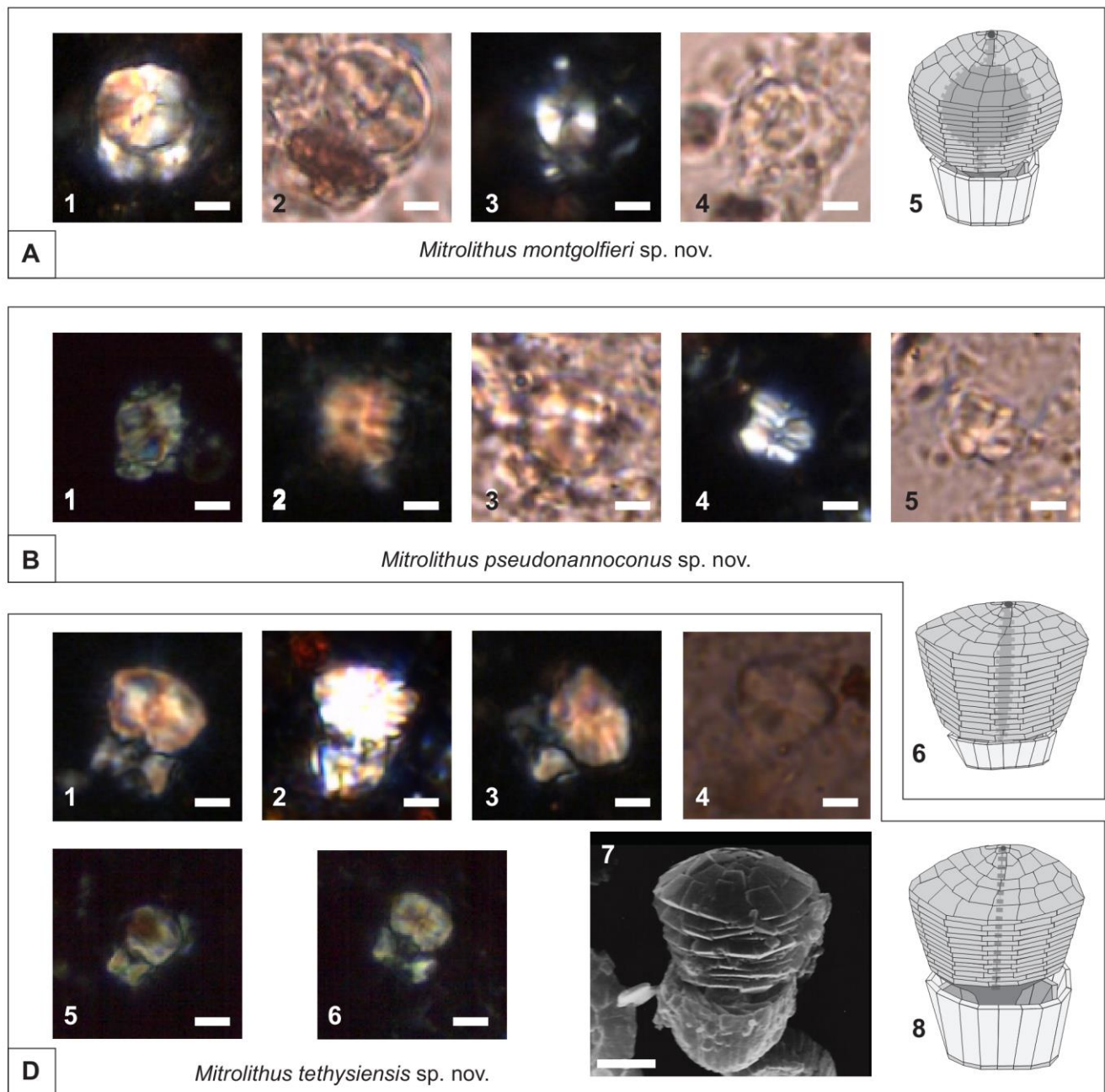


Figure 4. Micrographs showing the new species of *Mitrolithus* introduced in this work, as well as schematic drawing illustrating their main morphological features. The white scale bar is 2 μm .

(A) *M. montgolfieri*: 1 holotype in side-view with a small-sized basket like rim, under optical microscope, crossed polars (sample J.0-26); 2 specimen in side-view, with a small-sized basket like rim, under optical microscope crossed polars (sample J.0-28); 3 same specimen as 2 in parallel polars; 4 specimen in side-view, with a small-sized basket like rim, under optical microscope, crossed polars (sample J.0-28); 5 same specimen as 4 in parallel polars.

(C) *M. tethysiensis*: 1 holotype, side-view specimen under optical microscope, crossed polars (sample J.0-28); 2 side-view specimen under optical microscope, crossed polars (sample J.0-28); 3 side-view specimen under optical microscope, crossed polars (sample J.0-28); 4 same specimen as 3 in parallel polars; 5 specimen in side-view, with a smaller sized basket like rim, under optical microscope, crossed polars (sample J.0-28); 6 specimen in side-view, with a smaller sized basket like rim, under optical microscope, crossed polars (sample J.0-28); 7 schematic drawing side-view; 8 side-view in SEM of the specimen figured by Bown [8] from Timor (sample J237, micrograph UCL-2072-23).

5. Discussion

5.1. Calcareous nannofossil biostratigraphy

The calcareous nannofossil assemblage composition of the Kermanshah area clearly presents a South Tethyan affinity, given the richness in *Mitrolithus* species and the presence of *Mazaganella pulla* in the assemblage [8],[39]. The presence from the base of the J.1 member in the Kani Sad section of *M. lenticularis* allows dating the section to the NJT 3b nannofossil subzone of Mattioli and Erba [10] and Ferreira et al. [11] (Fig. 2; Table 2). This interval indicates a latest Sinemurian age for the J.1 member. A Sinemurian age is further supported by the sporadic presence of *P. marthae* in the J.1 member of Kani Sad section. This species is reported to disappear in the lower Sinemurian by Bown [8] and in the uppermost Sinemurian by Ferreira et al. [11]. *Parhabdolithus marthae* is therefore restricted to the Sinemurian. *Mazaganella* (*M. pulla* or *M. protensa*) has been sporadically recorded in the J.0 member of both Kani Sad and Sad sections; the NJT 3c subzone of Ferreira et al. [11] cannot be therefore identified. This subzone is thus merged into the NJT 3b-c (Fig. 2; Table 2).

The FO of the *Similiscutum* group is recorded in both sections in the shaly part of J.0 member (Fig. 2; Table 2). This peculiar event is consistently used by various authors to designate the NJT 4 zone (NJT 4a subzone) both in North-West and South-West Tethys regions [8],[10],[11]. The occurrence of *Similiscutum* is very relevant because the NJT 4a subzone can be used to detect the base of the Pliensbachian when other diagnostic fossils (e.g., ammonites) are lacking.

The new calcareous nannofossil biostratigraphy established here is partly in contrast with previous Pliensbachian to early Toarcian age assignments of the successions by means of radiolarians [1],[23],[24], and also allows reconsideration of the correct stratigraphic position of the lithological successions. In particular, based on calcareous nannofossil data, the J.1 and J.2 members of Abdi et al. [1],[23],[24] are in fact in an inverted position (Table 1). The new J.1 member used here (pelagic limestones and marls of previous J.2 of Abdi et al. [1],[23],[24] belongs to the upper Sinemurian NJT 3b subzone, whereas the new J.0 member made of cherts and shales (part of previous J.1 member of Abdi et al. [1],[23],[24] encompasses the uppermost Sinemurian NJT 3b-c subzone and the lowermost Pliensbachian NJT 4a subzone. The area is tectonically affected and the J.1 member is thrust over the J.0 member. In the lowermost part of J.1 member (J.2 in Abdi et al. [1],[23],[24]) of the Kani Sad section, the occurrence of the radiolarians *Praeconocaryomma bajaensis* sp. and *Bagotum modestum* sp. (which were used to interpret a Pliensbachian *p.p.* or early Toarcian age for this member) are compatible with an end-Sinemurian to earliest Pliensbachian age. In fact, *Bagotum modestum* first occurs in the UA 2 zone of Carter et al. [2], which spans the Sinemurian-Pliensbachian boundary. *Praeconocaryomma bajaensis* is also recorded from the lowermost Pliensbachian [2].

5.2. Evolutionary and palaeogeographic implications of the new *Mitrolithus* species

One of the most prominent features of the calcareous nannofossil assemblages of the Kermanshah area is the finding of a very common and diverse assemblage of *Mitrolithus* species (including three new ones), in the uppermost Sinemurian and lowermost Pliensbachian. In particular, two of the three newly described species have never been documented elsewhere but observed offshore Australia (Richard Howe, personal communication, 2019). Conversely, *M. tethysiensis* was previously reported by Bown [8] from a single Timor Island sample (J237), dated to as mid-Pliensbachian, but without any precise information about the age determination of the studied material. The absence of such species in classical and thoroughly studied localities of comparable age in western Tethys is intriguing. On the basis of the presence of endemic species, Bown [8] inferred a separate Pacific-Tethys Realm, including the south-eastern margin of Tethys to which the Kermanshah area belongs. However, no physical barrier is known between the eastern and the western Tethys (Fig. 1A, B), and most of the Lower Jurassic nannofossil species are known

to be cosmopolitan and successful throughout the marine environment [8]. Thus, at this stage it is difficult to explain such a limited distribution of the new *Mitrolithus* species. However, *M. jansae*, which is typically recorded at low-latitude Tethys sites [8], is considered to have behaved as a deep-dweller [40]–[42], thriving in the deep photic-zone in a way similar to the living species *Florisphaera profunda* [43]. If so, the intensity of sunlight irradiance was likely not sufficient at higher latitudes to support the development of *M. jansae* [39]. Also *F. profunda* abundance sharply decreases in between 30° and 40°N in the Pacific [43]. In this view, it is likely that the ecological requirements (in terms of light, nutrients, or other) of *M. montgolfieri*, *M. pseudonannoconus* and *M. tethysiensis* were only compatible with the low-latitude southeast margin of the Tethys. Alternatively, these species were likely not competitive enough with respect to other, well-established western Tethys species thriving in the deep photic-zone environment, such as *Crepidolithus crassus* [39],[44]–[49].

The spine morphologies of the newly described species are also very intriguing, in that they closely resemble the *Nannoconus* shape. *M. pseudonannoconus* sp. nov. has a reduced coccolith rim, with the spine dominating the coccolith (Fig. 4B), and isolated spines being commonly recorded. From a crystallographic point of view, the spines are made of calcite crystals with a plate c-axis, tangential to longitudinal axis of the spine. These crystals appear low birefringent when the spine is seen in distal view (Fig. 3A-6), while in side view the spine may present second-order orange colours (Fig 4A-1, B2, C1-3). This optical behaviour is very similar to *Nannoconus*, nannoliths, where the plate c-axes are arranged tangentially to the longitudinal axis. These morphological and crystallographic similarities between the spines of Lower Jurassic *Mitrolithus* species and Cretaceous *incertae sedis*, if not fortuitous, is very difficult to explain. However, both *Mitrolithus* and *Nannoconus* are well-known as having been typical components of Tethys nannoplankton assemblages. As for some *Mitrolithus* (e.g., *M. jansae*), a deep-dweller habitat has been inferred for nannoconids [50]. Thus, they might both represent organisms having independently adopted similar shapes in a process of morphological convergence. Interestingly, *Mitrolithus* (especially *M. jansae*) possesses a cone-like morphology strikingly similar to the Triassic genus *Eoconusphaera* and the Upper Jurassic/Lower Cretaceous genus *Conusphaera*, all being typically and abundantly recorded at low-latitudes in the Tethyan domain. Such a homeomorphy is puzzling because these taxa are recorded at present with mutually exclusive stratigraphic distributions [51]. The results of this paper showing homeomorphy for the inner core structures (i.e., the *Mitrolithus* spine) and the Cretaceous *Nannoconus* should enable a better overview of the evolution of conical calcareous nannofossils in the Mesozoic.

6. Conclusions

A common and diverse calcareous nannofossil assemblage is documented for the first time in this account from the Lower Jurassic shale, chert and pelagic limestone succession of the Kermanshah Basin (Kani Sad and Sad sections; western Iran; West Zagros). The new nannofossil record shown in this account and the re-examination of the range of radiolarian species challenge the former Pliensbachian to early Toarcian age assignment of the studied successions. In fact, the recorded radiolarian species turned out to be long-ranging taxa, whose earliest occurrence is consistent with the late Sinemurian-early Pliensbachian age provided by calcareous nannofossil assemblages and events. In particular, the last occurrence of *Parhabdololithus marthae* (a typical Sinemurian taxon) and the first occurrence of the *Similiscutum* group (lower Pliensbachian) allow the recognition in the two sections of the nannofossil subzones NJT 3b-c and NJT 4a. These results also allow a better understanding of the the stratigraphic position of the sedimentary units. In fact, the two studied sections represent the N and S limbs of a syncline over-thrusted by the radiolarite units.

710 Besides these stratigraphic and structural implications, the analysis of nannofossil
711 assemblages of the Kermanshah area revealed the presence of specimens of the genus *Mi-*
712 *trolithus* never described before, allowing the formal definition of three new species: *M.*
713 *montgolfieri*, *M. pseudonannoconus*, and *M. tethysiensis*. The two-former species present a
714 very peculiar morphology of the spine-structure infilling the central area of the coccolith,
715 and isolated spines resemble the morphology of Cretaceous nannoconids. Such records
716 addresses the question of morphological convergence or homeomorphy for two nannofos-
717 sil taxa (*Mitrolithus* and *Nannoconus*), which have a mutually exclusive stratigraphic dis-
718 tribution (Lower Jurassic and Cretaceous, respectively), but are both typical of low-lati-
719 tude, warm-water Tethyan settings. *Mitrolithus tethysiensis* was previously figured from a
720 single sample from Timor (Indonesia) and considered as a modified specimens of *M. ele-*
721 *gans*. The abundant record of *M. elegans* along with the three newly described species in
722 the Kermanshah area, and the fact that the new species have never been recorded in the
723 well-studied western Tethys settings support a strong endemism of calcareous nannofos-
724 sil assemblages in the Jurassic.

725
726
727
728
729
730
731
732
733
734
Acknowledgments: A preliminary version of this paper benefitted of insightful review and inspir-
ing comments by Paul R. Bown. We wish to warmly thank Mrs Ghislaine Broillet for preparation of
smear slides for calcareous nannofossil analysis and Zaminrizkavan Co. Ltd. for assistance during
fieldwork and petrographic studies. This work is a contribution to IGCP-655 project (UNESCO-
IUGS). Research of B. Bádenas is supported by Group E18: *Aragosaurus: Recursos Geológicos y Paleo-*
ambientales. Slides are curated at the Collections de Géologie de Lyon with the FSL N° from 769015
to 769091.

Appendix A

List of the species recorded or cited in this paper.

Alvearium dorsetense Black, 1965

Crepidolithus crassus (Deflandre in Deflandre and Fert, 1954) Noël, 1965

small-sized *Crepidolithus crassus* described in Suchéras-Marx et al. (2010)

Crepidolithus cavus Prins, 1969

Crepidolithus crucifer Rood et al. 1973

Crepidolithus granulatus Bown, 1987a

Crepidolithus impontus Grün et al., 1974

Crepidolithus timorensis Kristan-Tollmann, 1988

Crucirhabdus aff. *C. minutus* Jafar, 1983

Crucirhabdus primulus Prins 1969 ex Rood et al., 1973, emended Bown, 1987a

Mazaganella protensa Bown, 1987a

Mazaganella pulla Bown, 1987a

Mitrolithus elegans Deflandre in Deflandre and Fert, 1954

Mitrolithus jansae (Wiegand, 1984) Bown in Young et al., 1986

Mitrolithus lenticularis Bown, 1987a

Mitrolithus montgolfieri sp. nov.

Mitrolithus pseudonannoconus sp. nov.

Mitrolithus tethysiensis sp. nov.

Parhabdolithus liasicus subsp. *distinctus* Bown, 1987a

Parhabdolithus liasicus subsp. *liasicus* Bown, 1987a

Parhabdolithus marthae Deflandre in Deflandre and Fert, 1954

Parhabdolithus robustus Noël, 1965

Schizosphaerella spp. Deflandre and Dangeard, 1938

Similiscutum avitum de Kaenel and Bergen, 1993

Similiscutum cruciulus de Kaenel and Bergen, 1993

Similiscutum novum (Goy in Goy et al., 1979) Mattioli et al., 2004

Similiscutum orbiculus de Kaenel and Bergen, 1993

Similiscutum precarium de Kaenel and Bergen, 1993

Timorella cypella Bown, 1987a

Tubirhabdus patulus Rood, Hay and Barnard, 1973 ex Prins, 1969

References

- (1) Abdi, A.; Gharraie, M. H. M.; Bádenas, B. Internal Wave Deposits in Jurassic Kermanshah Pelagic Carbonates and Radiolarites (Kermanshah Area, West Iran). *Sediment. Geol.* **2014**, *314*, 47–59. <https://doi.org/10.1016/j.sedgeo.2014.10.006>.
- (2) Carter, E. S.; Goričan, Š.; Guex, J.; O'Dogherty, L.; De Wever, P.; Dumitrica, P.; Hori, R. S.; Matsuoaka, A.; Whalen, P. A. Global Radiolarian Zonation for the Pliensbachian, Toarcian and Aalenian. *Palaeogeogr. Palaeoclimatol. Palaeoecol.* **2010**, *297* (2), 401–419. <https://doi.org/10.1016/j.palaeo.2010.08.024>.
- (3) O'Dogherty, L.; Carter, E. S.; Dumitrica, P.; Goričan, Š.; Wever, P. D.; Bandini, A. N.; Baumgartner, P. O.; Matsuoaka, A. Catalogue of Mesozoic Radiolarian Genera. Part 2: Jurassic-Cretaceous. *Geodiversitas* **2009**, *31* (2), 271–356. <https://doi.org/10.5252/g2009n2a4>.
- (4) Barnard, T.; Hay, W.W. On Jurassic Coccoliths: A Tentative Zonation of the Jurassic of Southern England and North France. *Eclogae Geol. Helvetiae.* **1974**, *67*, 563–585.
- (5) Hamilton, G. B. Lower and Middle Jurassic Calcareous Nannofossils from Portugal. *Eclogae Geol. Helvetiae.* **1979**, *72*, 1–17.
- (6) Hamilton, G. B. Triassic and Jurassic Calcareous Nannofossils." A Stratigraphical Index of Calcareous Nannofossils. *Ellis Horwood Chichester.* **1982**, 17–39.
- (7) Medd, A. W. Medd, A.W. Nannofossil Zonation of the English Middle and Upper Jurassic Jurassic. *Mar. Micropaleontol.* **1982**, *7*, 75–95.
- (8) Bown, P. R. Taxonomy, evolution and biostratigraphy of Late Triassic-Early Jurassic calcareous nannofossils. *Special Papers in Palaeontology.* **1987a**, *38*, 1–118.
- (9) Bown, P. R.; Cooper, M. K. E.; Lord, A. R. A Calcareous Nannofossil Biozonation Scheme for the Early to Mid Mesozoic. *Newsl. Stratigr.* **1988**, 91–114. <https://doi.org/10.1127/nos/20/1988/91>.
- (10) Mattioli, E.; Erba, E. Biostratigraphic Synthesis of Calcareous Nannofossil Events in the Tethyan Jurassic. *Riv. Ital. Paleontol. E Stratigr.* **1999**, *105* (3), 343–376. <https://doi.org/10.13130/2039-4942/5380>.
- (11) Ferreira, J.; Mattioli, E.; Sucherás-Marx, B.; Giraud, F.; Duarte, L. V.; Pittet, B.; Suan, G.; Hassler, A.; Spangenberg, J. E. Western Tethys Early and Middle Jurassic Calcareous Nannofossil Biostratigraphy. *Earth-Sci. Rev.* **2019**, *197*, 102908. <https://doi.org/10.1016/j.earscirev.2019.102908>.
- (12) Cornée, J.-J.; Martini, R.; Villeneuve, R.; Zaninetti, L.; Mattioli, E.; Rettori, R.; Atrops, F.; Gunawan, W. Jurassic Pelagic Deposits of East Sulawesi (Kolonodale Area, Indonesia): New Biostratigraphic Data Based on Calcareous Nannofossils. *Geobios.* **1999**, *32*, 385–394.
- (13) Shafik, S.; Organisation, A. G. S. Significance of calcareous nannofossil-bearing Jurassic and Cretaceous sediments on the Rowley Terrace, offshore northwest Australia <https://researchdata.edu.au/significance-calcareous-nannofossil-northwest-australia/688200> (accessed Dec 9, 2021).
- (14) Kazmin, V.; Ricou, L.-E.; Sbertshikov, I. M. Structure and Evolution of the Passive Margin of the Eastern Tethys. *Tectonophysics* **1986**, *123* (1–4), 153–179. [https://doi.org/10.1016/0040-1951\(86\)90196-4](https://doi.org/10.1016/0040-1951(86)90196-4).
- (15) Bassoulet, J. P.; Elmi, S.; Poisson, A.; Cecca, F.; Bellion, Y.; Guiraud, R.; Baudin, F. Mid Toarcian. In: Atlas Tethys Palaeoenvironmental Maps; Dercourt, J., Ricou, L.E., Vrielynck, B. Eds.; No. BEICIP-FRANLAB, Rueil-Malmaison. **1993**, 63–84.
- (16) Robertson, A. H. F. Overview of Tectonic Settings Related to the Rifting and Opening of Mesozoic Ocean Basins in the Eastern Tethys: Oman, Himalayas and Eastern Mediterranean Regions. In: Imaging, Mapping and Modelling Continental Lithosphere Extension and Breakup; Karner, G, Manatschal, G, Pinheiro, L.M., Eds.; *Geol. Soc. Lond. Spec. Publ.* **2007**, *282* (1), 325–388. <https://doi.org/10.1144/SP282.15>.
- (17) Gharib, F.; De Wever, P. Radiolaires Mésozoïques de La Formation de Kermanshah (Iran). *Comptes Rendus Palevol* **2010**, *9* (5), 209–219. <https://doi.org/10.1016/j.crpv.2010.06.003>.
- (18) Navabpour, P.; Angelier, J.; Barrier, E. Brittle Tectonic Reconstruction of Palaeo-Extension Inherited from Mesozoic Rifting in West Zagros (Kermanshah, Iran). *J. Geol. Soc.* **2011**, *168* (4), 979–994. <https://doi.org/10.1144/0016-76492010-108>.
- (19) Berra, F.; Angiolini, L.; Muttoni, G. The Evolution of the Tethys Region throughout the Phanerozoic: A Brief Tectonic Reconstruction. In *Memoir 106: Petroleum Systems of the Tethyan Region*; Marlow, L., Kendall, C. C. G., Rose, L. A., Eds.; AAPG, **2014**, 1–27.
- (20) Mohajjel, M.; Fergusson, C. L.; Sahandi, M. R. Cretaceous–Tertiary Convergence and Continental Collision, Sanandaj–Sirjan Zone, Western Iran. *J. Asian Earth Sci.* **2003**, *21* (4), 397–412. [https://doi.org/10.1016/S1367-9120\(02\)00035-4](https://doi.org/10.1016/S1367-9120(02)00035-4).

21. (21) Abdi, A.; Bádenas, B.; Gharraie, M. H. M.; Gorican, S.; Toodekesht, S.; Mattioli, E. The Story of Kermanshah Radiolarite Basin from Early Jurassic to Late Cretaceous. 3rd Trigger International Conference. Institute for Advanced Studies in Basic Sciences, Zanjan, Iran, **2019**.
22. (22) Wrobel-Daveau, J.-C.; Ringenbach, J.-C.; Tavakoli, S.; Ruiz, G. M. H.; Masse, P.; Frizon de Lamotte, D. Evidence for Mantle Exhumation along the Arabian Margin in the Zagros (Kermanshah Area, Iran). *Arab. J. Geosci.* **2010**, *3* (4), 499–513. <https://doi.org/10.1007/s12517-010-0209-z>.
23. (23) Abdi, A. Sedimentology and Geochemistry of Kermanshah Radiolarite Complex with Special Reference to Depositional Environment, Doctoral-Ferdowsi University of Mashhad, Mashhad, **2016b**.
24. (24) Abdi, A.; Gharraie, M. H. M.; Bádenas, B. Radiolarian Productivity Linked to Climate Conditions during the Pliensbachian–Aalenian in the Kermanshah Basin (West Iran). *Facies* **2016a**, *62* (4). <https://doi.org/10.1007/s10347-016-0481-9>.
25. (25) Alavi, M.; Mahdavi, M. A. Stratigraphy and Structures of the Nahavand Region in Western Iran, and Their Implications for the Zagros Tectonics. *Geol. Mag.* **1994**, *131* (1), 43–47. <https://doi.org/10.1017/S0016756800010475>.
26. (26) Agard, P.; Omrani, J.; Jolivet, L.; Mouthereau, F. Convergence History across Zagros (Iran): Constraints from Collisional and Earlier Deformation. *Int. J. Earth Sci.* **2005**, *94* (3), 401–419. <https://doi.org/10.1007/s00531-005-0481-4>.
27. (27) Braud, J. *La Suture Du Zagros Au Niveau de Kermanshah (Kurdistan Iranien) : Reconstitution Paléogéographique : Évolution Géodynamique, Magmatique et Structurale*; Paris 11, **1987**.
28. (28) Bown, P. R.; Young, J. R. Techniques. In: Bown, P.R., Ed., *Calcareous Nannofossil Biostratigraphy* (British Micropalaeontological Society Publications Series), Chapman and Kluwer Academic, London. **1998**, 16–28.
29. (29) Roth, P. H. Roth, P.H. Preservation of Calcareous Nannofossils and Fine-Grained Carbonate Particles in Mid-Cretaceous Sediments from the Southern Angola Basin. In: Initial Reports of Deep Sea Drilling Project 75; Hay, W. W., Ed.; U.S. Government Printing Office, Washington, **1984**, 651–655.
30. (30) De Kaenel, E.; Bergen, J. A. New Early and Middle Jurassic Coccolith Taxa and Biostratigraphy from the Eastern Proto-Atlantic (Morocco, Portugal and DSDP Site 547 B). *Eclogae Geol. Helvetiae.* **1993**, *86* (3), 861–907.
31. (31) Mattioli, E.; Pittet, B.; Young, J. R.; Bown, P. R. Biometric Analysis of Pliensbachian-Toarcian (Lower Jurassic) Coccoliths of the Family Biscutaceae: Intra- and Interspecific Variability versus Palaeoenvironmental Influence. *Mar. Micropaleontol.* **2004**, *52* (1–4), 5–27. <https://doi.org/10.1016/j.marmicro.2004.04.004>.
32. (32) Bown, P. R.; Cooper, M. K. E. Jurassic. In: Bown, P. R. (Ed.) *Calcareous Nannofossil Biostratigraphy*. *Br. Micropalaeontological Soc. Publ. Ser.* **1998**, 34–85.
33. (33) Black, M. Coccoliths. *Endeavour.* **1965**, *24*, 131–137.
34. (34) Deflandre, G.; Fert, Ch. Observations Sur Les Coccolithophoridés Actuels et Fossiles En Microscopie Ordinaire et Électronique. *Annales de Paléontologie.* **1954**, *40* 115–176, pls. 1–15, text-figs. 1–127.
35. (35) Young, J. R.; Teale, C. T.; Bown, P. R. Revision of the Stratigraphy of the Longobucco Group (Liassic, Southern Italy); Based on the New Data on Nannofossils and Ammonite. *Eclogae Geologicae Helvetiae.* **1986**, *79*, 117–135..
36. (36) Prins, B. Evolution and Stratigraphy of Coccolithinids from the Lower and Middle Lias. In: *Proceedings I Int. Conf. Plankt. Microfossils*; Brönnimann, P. and Renz, P. Eds.; Genève, Switzerland,; **1969**, 547–558.
37. (37) Wiegand, G. Two Genera of Calcareous Nannofossils from the Lower Jurassic. *Journal of Palaeontology.* **1954**, *58*, 1151–1155.
38. (38) Casellato, C. E.; Erba, E. Calcareous Nannofossil Biostratigraphy and Paleoceanography of the Toarcian Oceanic Anoxic Event at Colle Di Sogno Section (Southern Alps, Italy). *Riv. Ital. Paleontol. E Stratigr.* **2015**, *121* (3), 297–327. <https://doi.org/10.13130/2039-4942/6520>.
39. (39) Mattioli, E.; Pittet, B.; Suan, G.; Mailliot, S. Calcareous Nannoplankton Changes across the Early Toarcian Oceanic Anoxic Event in the Western Tethys: Implications for Paleoceanography within the Western Tethys. *Paleoceanography* **2008**, *23* (3), A3208. <https://doi.org/10.1029/2007PA001435>.
40. (40) Bucefalo Palliani, R.; Mattioli, E. Ecology of dinoflagellate cysts and calcareous nannofossils from bituminous facies of the Early Toarcian, central Italy. *Proc. III EPA Workshop: Black Shales Models, Dotternhausen (Allemagne).* **1995**, 60–62.
41. (41) Erba, E. Calcareous Nannofossils and Mesozoic Oceanic Anoxic Events. *Mar. Micropaleontol.* **2004**, *52* (1–4), 85–106. <https://doi.org/10.1016/j.marmicro.2004.04.007>.
42. (42) Mattioli, E.; Pittet, B. Spatial and Temporal Distribution of Calcareous Nannofossils along a Proximal–Distal Transect in the Lower Jurassic of the Umbria–Marche Basin (Central Italy). *Palaeogeogr. Palaeoclimatol. Palaeoecol.* **2004**, *205* (3–4), 295–316. <https://doi.org/10.1016/j.palaeo.2003.12.013>.
43. (43) Okada, H.; Honjo, S. The Distribution of Oceanic Coccolithophorids in the Pacific. *Deep Sea Res. Oceanogr. Abstr.* **1973**, *20* (4), 355–374. [https://doi.org/10.1016/0011-7471\(73\)90059-4](https://doi.org/10.1016/0011-7471(73)90059-4).
44. (44) Bour, I.; Mattioli, E.; Pittet, B. Nannofacies Analysis as a Tool to Reconstruct Palaeoenvironmental Changes during the Early Toarcian Anoxic Event. *Palaeogeogr. Palaeoclimatol. Palaeoecol.* **2007**, *249* (1–2), 58–79. <https://doi.org/10.1016/j.palaeo.2007.01.013>.
45. (45) Fraguas, Á.; Erba, E. Biometric Analyses as a Tool for the Differentiation of Two Coccolith Species of the Genus *Crepidolithus* (Pliensbachian, Lower Jurassic) in the Basque-Cantabrian Basin (Northern Spain). *Mar. Micropaleontol.* **2010**, *77* (3–4), 125–136. <https://doi.org/10.1016/j.marmicro.2010.08.004>.

46. (46) Reggiani, L.; Mattioli, E.; Pittet, B.; Duarte, L. V.; Veiga de Oliveira, L. C.; Comas-Rengifo, M. J. Pliensbachian (Early Jurassic) Calcareous Nannofossils from the Peniche Section (Lusitanian Basin, Portugal): A Clue for Palaeoenvironmental Reconstructions. *Mar. Micropaleontol.* **2010**, *75* (1–4), 1–16. <https://doi.org/10.1016/j.marmicro.2010.02.002>.
47. (47) Suchéras-Marx, B.; Mattioli, E.; Pittet, B.; Escarguel, G.; Suan, G. Astronomically-Paced Coccolith Size Variations during the Early Pliensbachian (Early Jurassic). *Palaeogeogr. Palaeoclimatol. Palaeoecol.* **2010**, *295* (1–2), 281–292. <https://doi.org/10.1016/j.palaeo.2010.06.006>.
48. (48) Clémence, M.-E.; Gardin, S.; Bartolini, A. New Insights in the Pattern and Timing of the Early Jurassic Calcareous Nannofossil Crisis. *Palaeogeogr. Palaeoclimatol. Palaeoecol.* **2015**, *427*, 100–108. <https://doi.org/10.1016/j.palaeo.2015.03.024>.
49. (49) Ferreira, J.; Mattioli, E.; Pittet, B.; Cachão, M.; Spangenberg, J. E. Palaeoecological Insights on Toarcian and Lower Aalenian Calcareous Nannofossils from the Lusitanian Basin (Portugal). *Palaeogeogr. Palaeoclimatol. Palaeoecol.* **2015**, *436*, 245–262. <https://doi.org/10.1016/j.palaeo.2015.07.012>.
50. (50) Erba, E. Nannofossils and Superplumes: The Early Aptian “Nannoconid Crisis.” *Paleoceanography* **1994**, *9* (3), 483–501. <https://doi.org/10.1029/94PA00258>.
51. (51) Bown, P. R.; Cooper, M. K. E. Conical Calcareous Nannofossils in the Mesozoic. In: Nannofossils and Their Applications; Crux, J.A. and van Heck, S.E., Eds.; British Micropalaeontological Society Series, Ellis Horwood Ltd., Chichester. **1989**, 98–106..
52. (52) Blakey, R. C. Gondwana Paleogeography from Assembly to Breakup—A 500 m.y. Odyssey. In *Special Paper 441: Resolving the Late Paleozoic Ice Age in Time and Space*; Geological Society of America. **2008**, *441*, 1–28.
53. (53) Bown, P. R. The Structural Development of Early Mesozoic Coccoliths and Its Evolutionary and Taxonomic Significance. *Abhandlungen Der Geologischen Bundesanstalt.* **1987b**, *39*, 33–49.
54. (54) Menini, A.; Mattioli, E.; Spangenberg, J. E.; Pittet, B.; Suan, G. New Calcareous Nannofossil and Carbon Isotope Data for the Pliensbachian/Toarcian Boundary (Early Jurassic) in the Western Tethys and Their Palaeoenvironmental Implications. *Newsl. Stratigr.* **2019**, 173–196. <https://doi.org/10.1127/nos/2018/0476>.